Carbon Science

Vol. 2, No. 1 March 2001 pp. 15-21

Removal of Chromium by Activated Carbon Fibers Plated with Copper Metal

Soo-Jin Park♠ and Woo-Young Jung

Advanced Materials Division, Korea Research Institute of Chemical Technology, P.O. Box 107, Yusong, Taejon 305-600, Korea

♠e-mail: *psjin@pado.krict.re.kr*

(Received February 7, 2001; accepted February 31, 2001)

Abstract

In this work, activated carbon fibers (ACFs) were plated with copper metal using electroless plating method and the effects of surface properties and pore structures on chromium adsorption properties were investigated. Surface properties of ACFs have been characterized using pH and acid/base values. BET data with N_2 adsorption were used to obtain the structural parameters of ACFs. The electroless copper plating did significantly lead to a decrease in the surface acidity or to an increase in the surface basicity of ACFs. However, all of the samples possessed a well-developed micropore. The adsorption capacity of Cr(III) for the electroless Cu-plated ACFs was higher than that of the as-received, whereas the adsorption capacity of Cr(VI) for the former was lower than that of the latter. The adsorption rate constants (K_1, K_2, and K_3) were also evaluated from chromium adsorption isotherms. It was found that K_1 constant for Cr(III) adsorption depended largely on surface basicity. The increase of Cr(III) adsorption and the decrease of Cr(VI) adsorption were attributed to the formation of metal oxides on ACFs, resulting in increasing the surface basicity.

Keywords : *Activated Carbon Fibers, Adsorption, Chromium(III) and (VI), Rate Constant, Surface Functionality*

1. Introduction

Chromium compounds are present in the effluents of electroplating, metal finishing, magnetic tapes, wood preservation, leather tanning, pigments, and chemical manufacturing industries. They are one of the undesirable heavy metals because it affects human physiology, accumulates in the food chain and causes several ailments. Activated carbons (ACs) or activated carbon fibers (ACFs) have received great attentions as a adsorbent for chromium control because of their extended surface area, high adsorption capacity, uniform microporous structure, and specific surface reactivity [1, 2].

It is well known that the adsorption of chromium on ACFs is governed by structural parameters and surface functional groups, which can be changed by different treatments [3-5]. In real applications, there are many studies on the surface treatments to improve the surface and adsorption properties of ACs. Aggarwal *et al.* [6] studied the adsorption isotherms of Cr(III) and Cr(VI) ions on ACFs and granulated ACs after modifying their surfaces by oxidation with nitric acid, ammonium persulphate, hydrogen peroxide, and oxygen gas at 350°C. And they found that while the presence of acidic surface groups enhances the adsorption of Cr(III) cations, it suppresses that of Cr(VI) anions. Bautista-Toledo *et al.* [7] used the ACs treated with nitric acid to introduce surface oxygen complexes, observed that adsorption of both Cr(III) and Cr(VI) is enhanced by the presence of surface oxygen complexes of acid type on ACs. Park *et al.* [8, 9] modified ACs using chemical and electrochemical treatment method. They reported that these treatments can be utilized to develop more selective and effective adsorbents for gas and liquid pollution control. Perez-Candela *et al.* [10] studied in ACs, in powder and granular form, prepared from different raw materials, obtained by different activation procedures to remove Cr(VI) from aqueous. Recently, Park *et al.* [11] have reported that the amount of adsorption and adsorption rate of Cr(VI) increases with increasing the surface oxide groups of ACFs, even though both the specific surface area and the micropore volume do not significantly change on anodized ACFs.

It was also reported that the removal of Cr(III) and (VI) from aqueous solution by ACs depended on the pH and chromium concentration. Huang and Wu [12] revealed that the adsorption of Cr(VI) on ACs was highly pH-dependent and the maximum adsorption value was shown when pH was 6. Also, several researchers [13, 14] used activated carbons, lignite coal and bituminous coal for the adsorptive removal of chromium from aqueous solution at different pH values and observed that the adsorption of Cr(VI) was a maximum at pH = 3, while the reduction was a maximum at pH = 1.

The purpose of the present work is to investigate the surface properties and pore structure of the electroless Cu-plated ACFs, using pH, acid and base values, and BET

adsorption isotherms. It was tried to assess how these properties affect the adsorption capacity and rate of Cr(III) and Cr(VI).

2. Experimental

2.1. Materials

ACFs (TC-66E) used were supplied by Taiwan Carbon Co. The procedure of electroless copper plating on ACFs was described elsewhere [15]. In this work, four series of ACF samples were prepared according to the designed plating time. The ACFs studied were referred to as as-received, Cu/ACF-2 for 2 min plating time, Cu/ACF-5 for 5 min, and Cu/ACF-10 for 10 min.

2.2. Surface Properties and the content of copper

2.2.1. pH of ACFs

The pH of ACFs was measured according to the ASTM D 3838. About one gram of dry ACFs was added to 20 ml of distilled water, and the suspension was shaken overnight to reach equilibrium. The sample was filtered and the pH of the solution was measured.

2.2.2. Acid and base values

The density of the surface functional groups was determined by Boehms titration method [16]. In the case of acid value, about one gram of the sample was added to the beakers containing 100 ml of 0.1 N NaOH solution. The beakers were sealed and shaken for 24 h with purging N_2 gas, then the solution was filtered through a membrane filter (Φ = 0.45 ìm, nylon) and the excess of base was titrated with 0.1 N HCl. The acid value was calculated from the amount of hydrochloric acid that reacted with the sodium hydroxide. Likewise, the base value was determined by converse titration.

2.2.3. Content of copper

About 0.5 g of the sample was added to 30 ml of distilled water containing 5 ml of nitric acid and then boiled for 30 min. After cooling, the sample was filtered and the mixture was adjusted to the certain amount using a volumetric flask. The content of copper was determined by atomic absorption spectroscopy (AAS, Perkin-Elmer 2380).

2.3. Nitrogen adsorption

Nitrogen adsorption isotherms were measured using an ASAP 2400 (Micromeritics) at 77 K. Prior to each analysis, the samples were outgassed at 298 K for 6 h to obtain a residual pressure of less than 10^{-3} torr. The amount of nitrogen adsorbed on ACFs was used to calculate specific surface area and pore size distribution determined from BET equation [17] and BJH model [18], respectively. The following BET constant, C_{BET}, obtained by the intercept of the BET equation can be used for the calculation of the net of heat adsorption (NHA):

$$C_{BET}=\exp\left[\frac{E_0 - E_L}{RT}\right] \quad (1)$$

where C_{BET} is characteristic constant of the adsorbate-adsorbent, E_0 the heat of adsorption in the first layer, E_L the heat of liquefaction, R the gas constant, and T the Kelvin temperature.

Also, the DR equation was applied to the nitrogen experimental isotherms for micropore analysis [19]. A liquid density of 0.808 g/cm^3 was assumed for nitrogen in the adsorbed phase at 77 K in order to calculate micropore volumes [20]. Assuming a slit-shaped pore, the micropore half-width, x, may be calculated using the following equation:

$$x = \beta\kappa/E \quad (2)$$

where β is an affinity coefficient, E a characteristic adsorption energy, and k a constant. For nitrogen, β is equal to 0.35, and k to 13 nm kJ/mol for this set of materials [22].

2.4. Adsorption of Chromium

The adsorption isotherms of Cr(III) and Cr(VI) on ACFs were obtained by using stopper flasks containing 0.1 g of ACFs in 100 ml of aqueous solution of sodium chromate ($Na_2CrO_4 \cdot 4H_2O$) and chromium chloride ($CrCl_3 \cdot 6H_2O$), respectively. In the case of Cr(VI) adsorption, the initial pH of the solution was adjusted to about 3 using 0.1 N HCl and 0.1 N NaOH. The bottles were sealed with glass stopper and then shaken for a given time (10, 20, 30, 40, 50, 60, 120, and 180 min) at 25°C at a frequency of 95 strokes/min using a thermostatic shaking bath. At the end of the reaction period, each reaction mixture was filtered to separate the supernatants and ACFs. The amount of chromium adsorbed was determined by atomic absorption spectroscopy (AAS, Perkin-Elmer 2380). All isotherms have been carried out without adding any buffer to control the pH in order to avoid the introduction of a new electrolyte in the system, which may influence the adsorption process [7].

3. Results and Discussion

3.1. Surface Properties and content of copper

Table 1 summarizes the experimental surface properties and copper content of ACFs determined by pH, Boehm's titration and AAS. The surface of the as-received was acidic, probably due to its origin and the method of activation. However, data in Table 1 show that the electroless copper plating does significantly lead to a decrease in the surface acidity and an increase in the surface basicity in this system, indicating that the basic species are created on the surface of ACFs [21]. The results obtained from acid/base titration were in general agreement with the pH values. Also, this behavior of the surface basicity was similar as that of copper content; the content of copper increased with increasing the

Table 1. Surface properties of the ACFs studied and copper content

Nomenclature	pH	Acidic values [meq/g]	Basic values [meq/g]	Copper content [ppm]
as-received	4.24	440	20	0
Cu/ACF-2	8.57	150	260	43
Cu/ACF-5	10.27	70	300	98
Cu/ACF-10	10.43	60	310	102

plating time. It clearly indicated that the increase of the surface basicity as compared to the as-received was likely due to the increase in the basic species via the introduction of copper metal on ACFs.

3.2. Nitrogen adsorption

Very little previous work has been reported to demonstrate how electroless copper plating affects the pore structure of ACFs. An understanding of the specific surface area and porosity of an adsorbent can be achieved by the construction of an adsorption isotherm. The results of nitrogen adsorption isotherms of the ACFs deposited with and without copper metal are shown in Fig. 1. As a result, all of the samples had approximately the Type I isotherms having well-developed micropores according to the BET's classification [17]. It is well known that adsorption on microporous carbons leads to an isotherm of Type I and that the microporous solid of wider micropore diameter of molecular dimensions shows Type Ib character coming to saturation at a lower P/P_0 [22, 23]. For the electroless Cu-plated ACFs, all isotherms are almost identical and have round knees around $0.01 < P/P_0 < 0.1$ with a gradual approach to the plateau. The similar adsorption shape suggests uniform in the pore structure [24].

The distribution of pore sizes calculated from BJH model is presented in Fig. 2. The analysis of the data indicates that

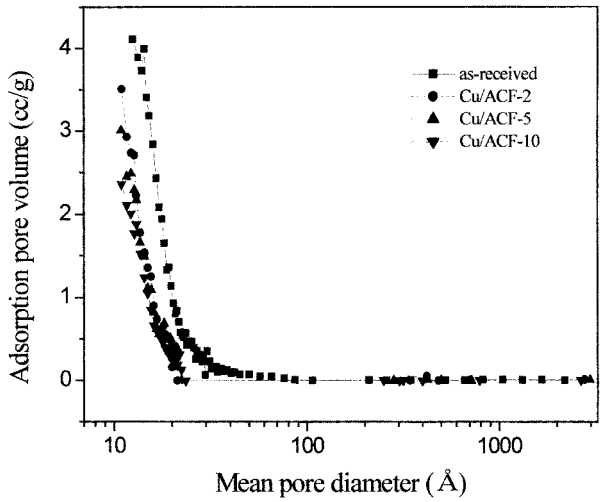

Fig. 2. Pore size distribution of various samples.

electroless copper plating causes changes mainly in the population of mesopores. The carbons as-received have a little mesopore larger than 20 Å, whereas electroless Cu-plated ACFs have not. The disappearance of mesopores is probably due to an alteration of the carbon surface by means of the introduction of copper and the formation of copper oxides [25].

As mentioned in the experiment section, micropore filling of vapors can be described using the Dubinin-Radushkevich equation. Fig. 3 shows the DR-plots for the N_2 adsorption on ACFs. These plots exhibit good linear relationships in the lower pressure range ($\ln^2(P_0/P) > 10$), indicating that the micropore filling of N_2 is nearly completed at this region [23].

The structural parameters and net heat of adsorption calculated from nitrogen adsorption isotherms are listed in Table

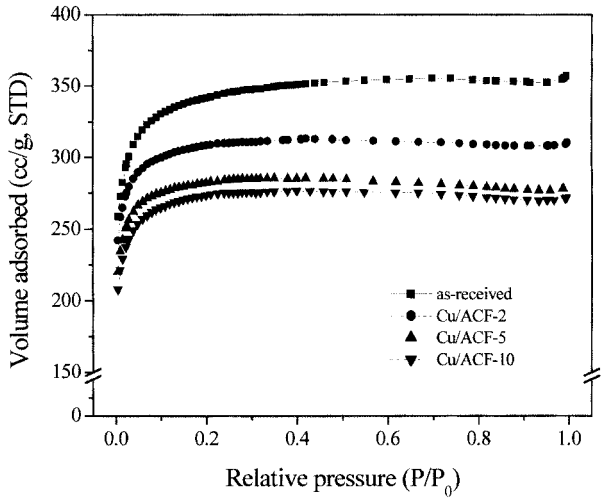

Fig. 1. Nitrogen adsorption isotherms at 77K for the ACFs studied.

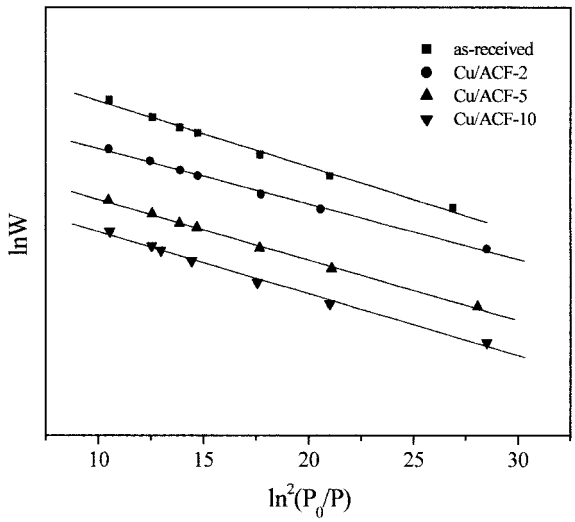

Fig. 3. DR-plots for the nitrogen adsorption on ACFs.

Table 2. Structural parameters of the ACFs studied and net heat of adsorption

Nomenclature	S_{BET} [m^2/g]	V_{mic} [cm^3/g]	*L* [Å]	NHA [kJ/mol]
as-received	1,334	0.54	14.4	4.20
Cu/ACF-2	1,213	0.49	13.0	4.51
Cu/ACF-5	1,110	0.45	13.5	4.44
Cu/ACF-10	1,056	0.43	13.8	4.30

2. The introduction of copper metal on ACFs influences the decrease in surface areas and micropore volumes of the samples as shown in Figs. 1 and 2. As expected, it is noted that the micropore volume and specific surface area are linearly proportional to each other such that the specific surface area decreases with decreasing micropore volume [26, 27]. However, it is revealed that the lowest micropore diameter (*L*) is obtained for Cu/ACF-2 and the highest for the as-received. Electroless copper plating may block the mesopores of the as-received. Additional plating process may also cause the additional blocking of these blocked mesopores, resulting in decreasing the population on micropores [28].

Meanwhile, the net heat of adsorption is the highest for Cu/ACF-2, even though the specific surface area of Cu/ACF-2 is lower than that of the as-received. It is accepted that average size of micropores is related to the net heat of adsorption determined from BET constant [29-31]. The BET "C" values are obtained in the range of relative pressure between 0.01 and 0.1. As expected, the net heat of adsorption increased as the average size of micropores decreased. Dependence of NHA on the micropore diameter is plotted in Fig. 4. The correlation is clearly seen with the coefficient of regression (R) is equal to 0.995. This behavior is due to the overlapping of the adsorption potentials from the walls of the micropores [5, 29-31].

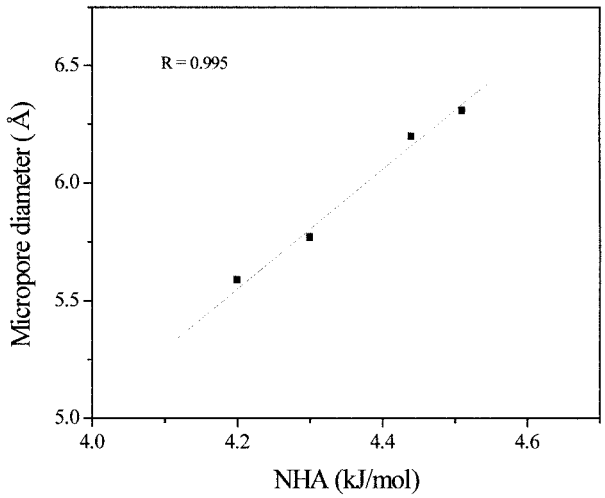

Fig. 4. Dependence of NHA on the micropore diameter.

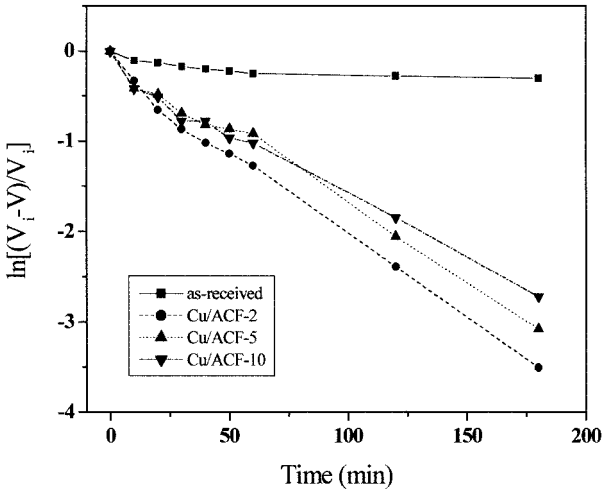

Fig. 5. Variation of Cr(III) concentration as a function of time on ACFs (V_i: initial concentration of Cr(III), V: amount adsorbed in a designed time).

3.3. Adsorption of Cr(III) and (VI)

The results of adsorption rates of Cr(III) ions from aqueous solutions of chromium chloride in the concentration of 50 mg/l on the samples are shown in Fig. 5. The final pH values of the solution are less than 4.5 in this experiment. It was seen that the concentration of Cr(III) adsorbed on the as-received was much less than those on the Cu-plated samples, although the specific surface area of the as-received is higher than those of the plated with Cu.

Cr(III) ions in aqueous solutions exist as $[Cr(H_2O)_6]^{3+}$. These associated water molecules around the Cr(III) ions are exchanged with the hydroxyl ions, the number exchanged depending upon the pH of the solution [32]. Thus, a change in pH of the solution will change the extent of the positive charge on the chromic ion. These changes in the negative charge on the carbon surface as a result of electroless plating and the changes in the positive charge on the Cr(III) ions in solution favor the adsorption of Cr(III) ions because the electrostatic attractive interactions between the carbon surface and the chromium ions present in the solution are enhanced. These results indicate the chemical nature of the adsorbent has more influence than the surface area and porosity of the adsorbents [7, 33].

Also, the results of adsorption rates of Cr(VI) ions from aqueous solutions of sodium chromate in the concentration of 53 mg/l on the samples are shown in Fig. 6. It is shown that the adsorption behaviors of Cr(VI) are greatly different from those of Cr(III) under similar conditions. The adsorption capacity of the samples as-received is inferior to that of the electroless Cu-plated ACFs in the Cr(III) ion adsorption. Whereas, the former is superior to the latter in the adsorption case of Cr(VI) ions. This difference may be attributed to the fact that Cr(VI) has a state of $HCrO_4^-$ or $Cr_2O_7^{2-}$ in the pH

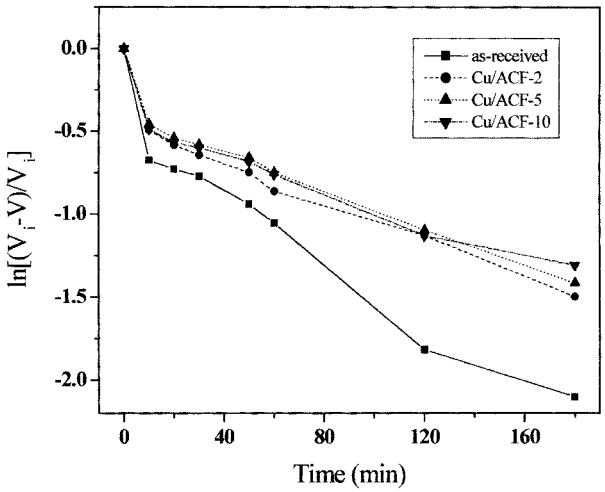

Fig. 6. Variation of Cr(VI) concentration as a function of time on ACFs (V_i: initial concentration of Cr(VI), V: amount adsorbed in a designed time).

range 2-6 in the aqueous solution [32]. The electroless Cu-plated samples have more the non-acidic or basic surface oxygen complex than the samples as-received. Thus, there is little or no existence of some positively charged sites where negatively charged Cr(VI) ions can be adsorbed, resulting in decreasing the adsorption of Cr(VI) ions.

3.4. Chromium adsorption rate

The adsorption rate of adsorbates can be expressed as K_1, K_2 and K_3 constants as shown in Fig. 7, which are calculated from the slope of the best fit line of the amount adsorbed as a function of adsorption time according to the following equation [34]:

$$\ln[(V_i - V)/V_i] = K_n t + C \quad (3)$$

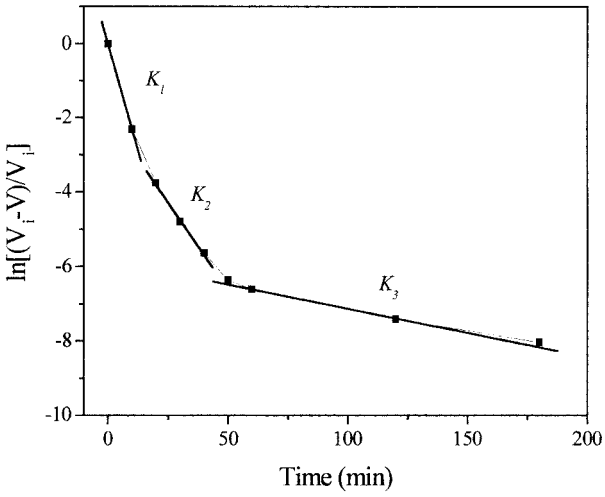

Fig. 7. Determination of adsorption rate constants for Cr(III) and Cr(VI).

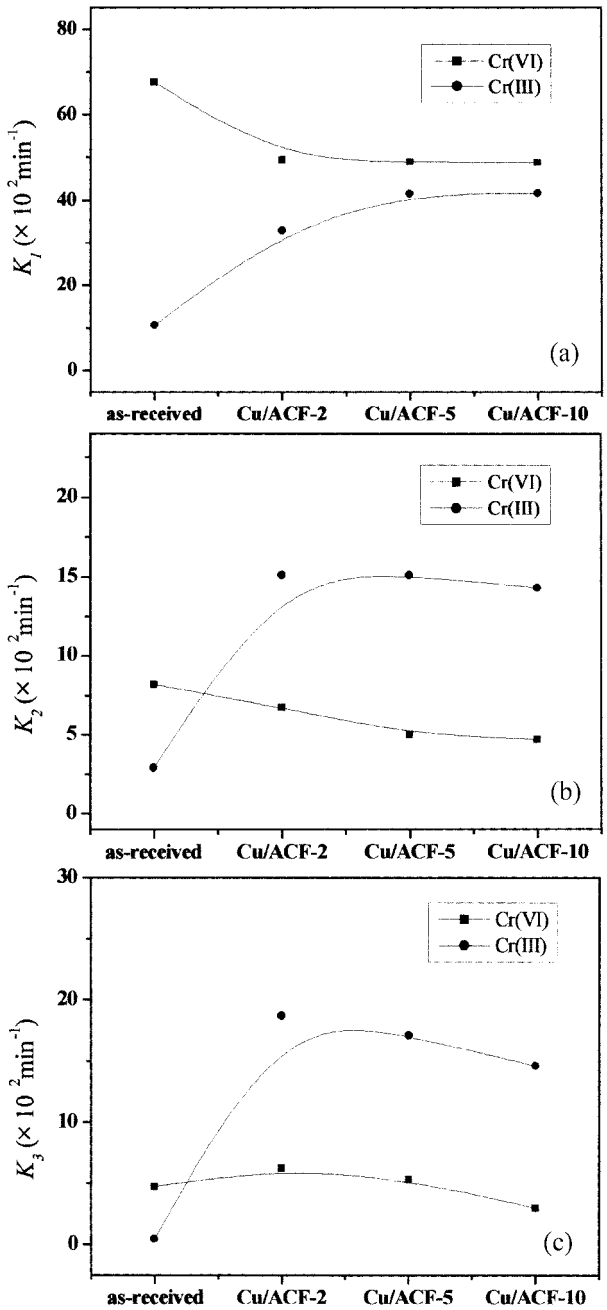

Fig. 8. Variation of K_1, K_2 and K_3 adsorption rate constants of the ACFs studied for Cr(III) and (VI).

where K_n is rate constant, t time in min, and C Y-intercept.

Fig. 8 shows the variation of K_1, K_2 and K_3 constants of adsorption for Cr(III) and (VI) derived from Figs. 5 and 6. As expected, the electroless copper plating leaded to an increase in K_1 constant for Cr(III) adsorption, or to a decrease for Cr(VI) as compared with the as-received. It was noted that for Cr(III) adsorption on the treated ACFs, K_1 constant increased as the plating time increases, while K_2 and K_3 decrease. The behavior of K_1 constant was in agreement with

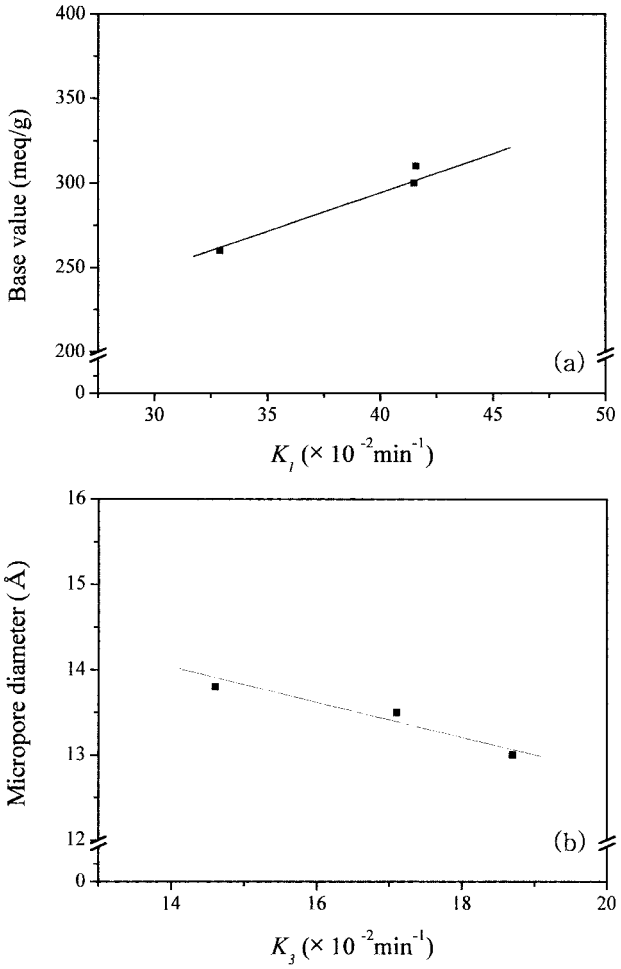

Fig. 9. Dependence of K_1 constant on surface basicity (a) and K_3 on micropore diameter (b).

that of base values, but for K_2 and K_3 are not. It suggested that the specific chemical interaction is the major mechanism responsible for the adsorption process for K_1. In order to assess the effects of surface properties and micorpore diameter on chromium adsorption rate, these relationships could be plotted as seen in Fig. 8. It is shown that K_1 constant depends on surface basicity (Fig. 9(a)), while K_3 constant on micropore diameter (Fig. 9(b)). It was indicated that the average size of the micropores is more contributing factor than surface properties for K_3.

4. Conclusion

In this work, the effects of surface properties and pore structure of Cu-plated ACFs on chromium adsorption were investigated. The introduction of copper metal on ACFs significantly leaded to an increase in the surface basicity, resulting in increasing the adsorption capacity of Cr(III) from aqueous solutions regardless of a decrease in surface area. It was then concluded that the adsorption of chromium ions was essentially dependent on surface properties, rather than by the surface area and porosity of the solid in the context of adsorption amount and rate measurements.

Acknowledgement

This work was supported by grant No. 2000-2-30100-011-3 from the Basic Research Program of the Korea Science & Engineering Foundation.

References

[1] Cheremisinoff, P. M.; Ellerbusch, C. *"Carbon Adsorption Handbook"*, Ann Arbor Science, Ann Arbor, Michigan, 1978.
[2] Bansal, R. C.; Donnet, J. B.; Stoeckli, F. *"Active Carbon"*, Dekker, New York, 1988, 27.
[3] Park, S. J. *"Interfacial Force and Fields: Theory and Applications"*, ed. J. P. Hsu, Dekker, New York, 1999.
[4] Park, S. J.; Donnet, J. B. *J. Colloid Interface Sci.* **1998**, *200*, 46.
[5] Lowell, S.; Shields, J. E. *"Powder Surface Area and Porosity"*, Chapman & Hall, London, 1991.
[6] Aggarwal, D.; Goyal, M.; Bansal, R. C. *Carbon* **1999**, *37*, 1989.
[7] Bautista-Toledo, I.; Rivera-Utrilla, J.; Ferro-Garcia, M. A.; Moreno-Castilla, C. *Carbon* **1994**, *32*, 93.
[8] Park, S. J.; Kim, K. D. *J. Colloid Interface Sci*. **1999**, *212*, 186.
[9] Park, S. J.; Kim, K. D. *J. Colloid Interface Sci*. **1999**, *218*, 331.
[10] Perez-Candela, M.; Martin-Martinez, J. M.; Torregrosa-Macia, R. *Water Res*. **1995**, *29*, 2174.
[11] Park, S. J.; Park, B. J.; Ryu, S. K. *Carbon* **1999**, *37*, 1223.
[12] Huang, C. P.; Wu, M. H. *Water Res.* **1977**, *11*, 673.
[13] Narayana, N.; Krishnaiah, A. *Indian J. Environ. Protec.* **1989**, *9*, 30.
[14] Huang, C. P.; Wu, M. H. *J. Water Pollut. Control Fed.* **1975**, *47*, 2437.
[15] Park, B. J.; Park, S. J. *J. Mater. Sci. Lett*. **1999**, *18*, 1607.
[16] Boehm, H. P. *Adv. Catal*. **1966**, *16*, 179.
[17] Brunauer, S.; Emmett, P. H.; Teller, E. *J. Am. Chem. Soc.* **1938**, *60*, 309.
[18] Barrett, E. P.; Joyner, L. C.; Halenda, P. H. *J. Am. Chem. Soc*. **1951**, *73*, 373.
[19] Dubinin, M. M. *Chem. Rev.* **1960**, *60*, 235.
[20] Dubinin, M. M.; Stoeckli, H. F. *J. Colloid Interface Sci.* **1980**, *75*, 34.
[21] Adib, F. J.; Bagreev, A.; Bandosz, T. J. *Environ. Sci. Technol.* **2000**, *34*, 686.
[22] Rodriguez-Reinoso, F.; Garrido, J.; Martin-Martinez, J.

M.; Molina-Sabio, M.; Torreyrosa, R. *Carbon* **1987**, *27*, 23.
[23] Matsumoto, A.; Zhao, J. X.; Tsutsumi, K. *Langmuir* **1997**, *13*, 496.
[24] Salame, I. I.; Bandosz, T. J. *Ind. Eng. Chem. Res.* **2000**, *39*, 301.
[25] Salame, I. I.; Bandosz. T. J. *J. Colloid Interface Sci*. **1999**, *210*, 367.
[26] Barton, S. S.; Evans, M. J. B.; MacDonald, J. A. F. *Adsorption Sci. Technol*. **1993**, *10*, 75.
[27] Mangun, C. L.; Benak, K. R.; Daley, M. A.; Economy, J. *Chem. Mater.* **1999**, *11*, 3476.
[28] Daley, M. A.; Tandon, D.; Economy, J. *Chem. Mater.* **1996**, *34*, 377.
[29] Dubinin, M. M. *Carbon* **1989**, *27*, 457.
[30] Dubinin, M. M. "*Chemistry and Physics of Carbon*", Vol. 2, ed. P. L. Walker Jr., Dekker, New York, 1966.
[31] Nguyen, C.; Do, D. D. *Langmuir* **1999**, *15*, 3608.
[32] Cotton, F. A.; Wilkison, G. "*Advanced Inorganic Chemistry*", 5th ed. Wiley, New York, 1998.
[33] Bagreev, A.; Adib, F.; Bandosz, T. J. *J. Colloid Interface Sci*. **1999**, *219*, 327.
[34] Kushiro, K.; Oda, H.; Yokokawa, C. *Tanso* **1991**, *148*, 151.